ANALYSIS OF THE PROCESS BEHAVIOR FOR PLANETARY ROLLER EXTRUDERS

Rudloff Johannes (1), Lang Marieluise (1), Kretschmer Karsten (1), Heidemeyer Peter (1), Bastian Martin (1), Koch Michael (2)

(1) SKZ - German Plastics Center - Würzburg - Germany
(2) KTI - Kunststofftechnik Ilmenau - Ilmenau - Germany

ABSTRACT

In the last few years process models for the planetary roller extruders were developed. These models are allowing an estimation of the processes in the extruder for the first time. However, because of the simplifications that were used for modeling, there can be considerable differences between simulated and experimental results. In this paper, a dimensionless approach for modeling the planetary roller extrusion process is proposed to improve the model quality. Therefore experimental trials with a variation of extruder configuration, material type, throughput and screw speed had been conducted. At these experiments the pressure build up was determined. Based on the results drag flow rate and pressure flow rate were expressed as dimensionless operating numbers to show the influence of power law index and geometry on the pressure building capacity of the extruder. This can help to find more precise assumptions for the process models.

Index Terms - Compounding, Extrusion, Planetary Roller Extruder, Simulation, Modeling

1. INTRODUCTION

The planetary roller extruder (PRE) was developed more than 50 years ago for the compounding of PVC. This extruder type is well known for its superior mixing performance and its exact temperature control capabilities. Therefore it is widely used in the polymer industry for the compounding of shear- and temperature sensitive materials like PVC [1] or Wood Plastic Composites [2]. Beside this, the extruder is used in the chemical, pharmaceutical and food industry for a broad variety of compounding and processing applications. In contrast to the considerable amount of scientific work that deals with investigation, modeling or simulation of the process behavior of single and twin screw extruders [e. g. 3-7] there are only a few publications about planetary roller extruders [8, 9]. Due to increased quality requirements and the trend to cost reduction by process optimization, this is increasingly becoming a problem for plant construction and processing companies. In order to counteract this tendency, first process models for the planetary roller extruders were developed in our former work [10, 11]. These models deliver an estimated insight into the processes of the extruder for the first time. However there can be considerable differences between simulated and experimental results, which result from required simplifications that were used for modeling. Our purpose in this paper is to take a closer look on the melt transport in fully filled sections of the PRE for reducing these differences.

2. FUNCTIONAL PRINCIPLE OF PRE

A schematically view of the PRE is shown in Figure 1. The first step in a common process is to charge the material into the extruder. Then the material enters the feeding section (1) that is basically similar to a solid conveying section of the single screw extruder concept. The main difference to single screw extruders is, that PRE as compounding extruders are usually operated in starved fed conditions. The sole function of the filling section is to transport the solid particles into the following planetary roller section (2a). This section is similar to planetary gears with a large length and a 45 ° helical gearing angle. It consists of a central spindle, a variable number of planetary spindles within a barrel with an internal gearing. The main spindle, which is connected to the "single screw" of the feeding section, is driven by the motor. Due to the gearing of the main spindle and the internal gearing of the barrel, the rotation and thus the torque of the main spindle is distributed to the planetary spindles and makes those rotate. The helical gearing causes both a rolling motion similar to a rolling mill and axial transporting of the material. At the end of a planetary roller section the material can be conveyed to further downstream equipment as e.g. a die, an open end-plate, a pelletizing unit or a melt pump (3). The downstream equipment builds up a pressure that has to be provided by the extruder. This leads to a fully filled section at the end of the planetary roller section (2b). The pressure depends e.g. on the material parameters, the mass temperature, the throughput and the geometry of the downstream flow channels.

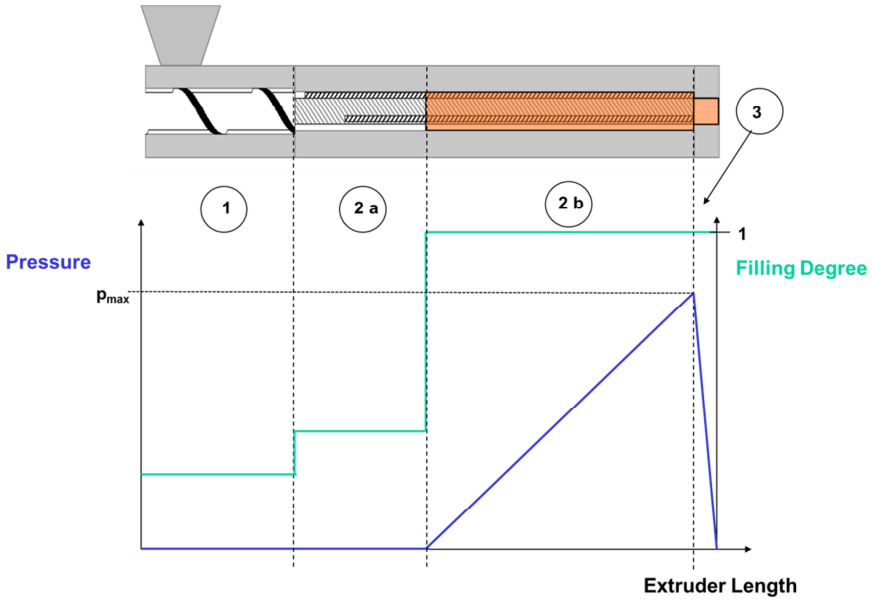

Figure 1: Schematically view of a PRE processing unit with feeding section (1), partial filled planetary roller section (2a), fully filled planetary roller section (2b) and die (3)

3. EXPERIMENTAL

To visualize the influence on the pressure build up, experimental trials with an ENTEX planetary roller extruder TP-WE 70 had been conducted. During the experiments the parameters extruder configuration, material type, throughput and screw speed were varied. The chosen materials for the investigation were LLDPE type LyondellBasell Luflexen 18, HDPE type Sabic PE 6060 and PS type BASF PS 143E. The flow curves of the materials at a

temperature of 200 °C were measured with a high pressure capillary rheometer type Göttfert Rheograph 6000 and are shown in Figure 2.

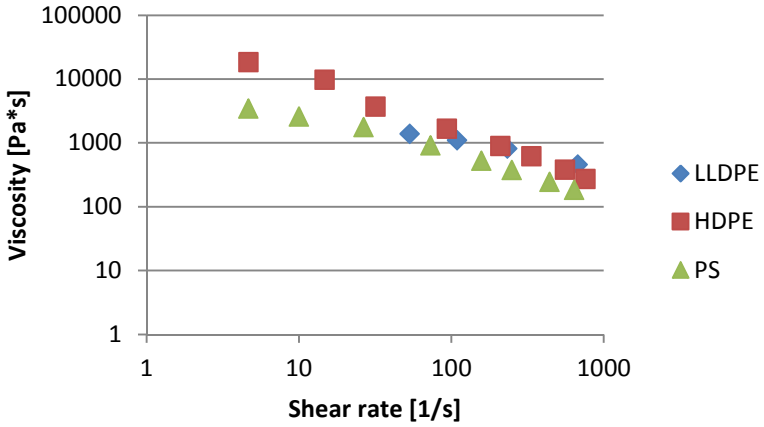

Figure 2: Viscosity over shear rate for the investigated materials

In order to determine the pressure build up a special barrel was used which can be opened. After reaching a steady state operation condition, the pressure at the extruder die was measured, then the machine was stopped abruptly and the barrel was opened. Thereby the length of the fully filled section could be determined (Figure 3).

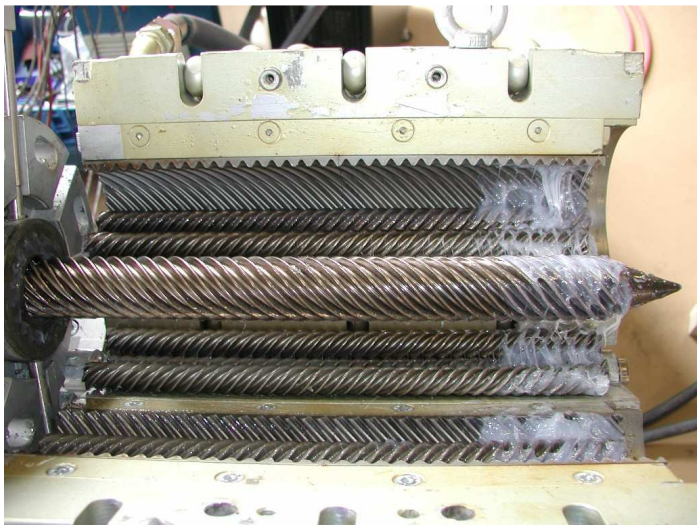

Figure 3: Opened barrel of the PRE experimental plant

4. RESULTS AND DISCUSSION

For the dimensionless analyses of the flow in the fully filled section it is assumed, that the material transport takes place in a number of parallel channels, which are formed between two planetary spindles, the main spindle and the barrel. Therefore the geometry is transformed into individual rectangular channels as shown in Figure 4.

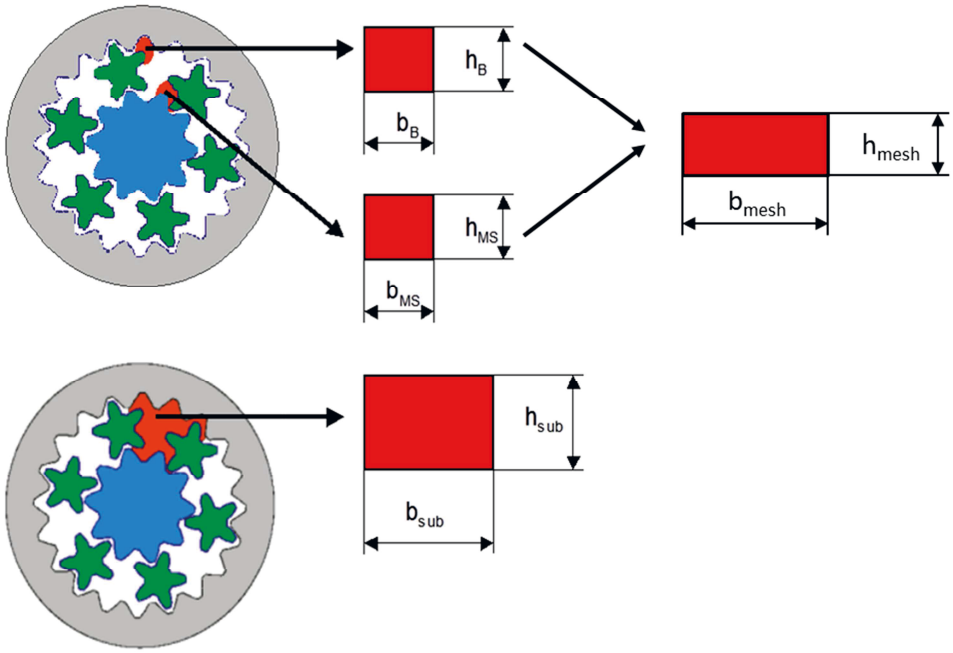

Figure 4: Rectangular channels for describing the material transport

There are two small channels based on the intermeshing sections between the teeth of the spindles and a larger channel based on the free volume sections between the center axes of the rollers. In the next step the two small channels in the intermeshing section are joined to one channel with a width b_{mesh} and an average height h_{mesh}.

$$h_{mesh} = \frac{h_{MS} + h_B}{2} \tag{1}$$

$$b_{mesh} = b_{MS} + b_B \tag{2}$$

where h_{MS} is the height of a tooth at the main spindle, h_B is the height of a tooth at the barrel and b_{MS} as well as b_B are the average diameter of a planetary spindle. The height of the large channel h_{sub} is given by the difference between the average main spindle and barrel diameters. With the free cross sectional area in the extruder A_{free} and the number of planetary spindles n_{pl} the width of the channel b_{sub} is calculated

$$b_{sub} = \frac{\frac{A_{free}}{n_{pl}} - h_{mesh} \times b_{mesh}}{h_{sub}} \tag{3}$$

Regarding the material transport in the fully filed section it is assumed that the volume flow given by the dosing unit $\dot{V}$ has to be the sum of the volume flow in the channels

$$\frac{\dot{V}}{n_{pl}} = \dot{V}_{mesh} + \dot{V}_{sub} \tag{4}$$

and that the pressure difference in z direction is equal in the channels

$$\frac{\Delta p}{\Delta z} = \frac{\Delta p_{mesh}}{\Delta z_{mesh}} = \frac{\Delta p_{sub}}{\Delta z_{sub}} \tag{5}$$

Furthermore it is assumed that material transport is affected by a superposition of drag and pressure flow as it is known for most extruders. According to that approach a dimensionless volume flow number and a dimensionless pressure gradient number are defined. The dimensionless volume flow $\pi_{\dot{V}}$ is calculated with the volume flow given by the dosing unit divided by the maximal drag volume flow in the intermeshing section channels

$$\pi_{\dot{V}} = \frac{\dot{V}}{n_{pl} \frac{1}{2} \cdot h_{mesh} \cdot b_{mesh} \cdot v_z} \tag{6}$$

where v_z is the average melt velocity in the intermeshing section channels as described by Limper [8]. To get a dimensionless pressure gradient π_p , the pressure induced volume flow is divided by the maximal drag volume flow in the intermeshing section channels

$$\pi_p = \frac{\Delta p}{\Delta z} \cdot \frac{h_{mesh}^{n+1}}{6 \cdot K \cdot v_z^n} \tag{7}$$

where the flow exponent *n* and the flow consistency index *K* are used to describe the viscosity according to the Ostwald–de Waele relationship. The values for the three materials are shown in table 1.

Table 1: Viscosity data of the used materials

Material	Flow exponent n [-]	Flow consistency index K [Pa*s]
LLDPE	0,63	5973
HDPE	0,17	72144
PS	0,52	7533

The dimensionless operating numbers calculated with the experimental data are shown in Figure 5. A change of the dimensionless volume flow has only minor influence on the dimensionless pressure gradient for most process points. The dimensionless pressure gradient varies in a range of 0,1 to 0,3. This corresponds to the known poor pressure build up capability of the PRE. The reason for that is a pressure flow from the die to the filling section in the large channels that has to be compensated by the drag flow in the intermeshing section channels. Furthermore there is one process point for all three materials that has a much lower pressure gradient. This process point was carried out with three planetary spindles, so that the width of the large channel and thus the backwards orientated pressure flow increased. A distinct influence of the flow exponent cannot be ascertained, but it seems that the pressure build up gets better with lower flow exponents. This occurs, if the influence of the flow exponent on the material flow in the large channels is higher than on the flow in the intermeshing section channels.

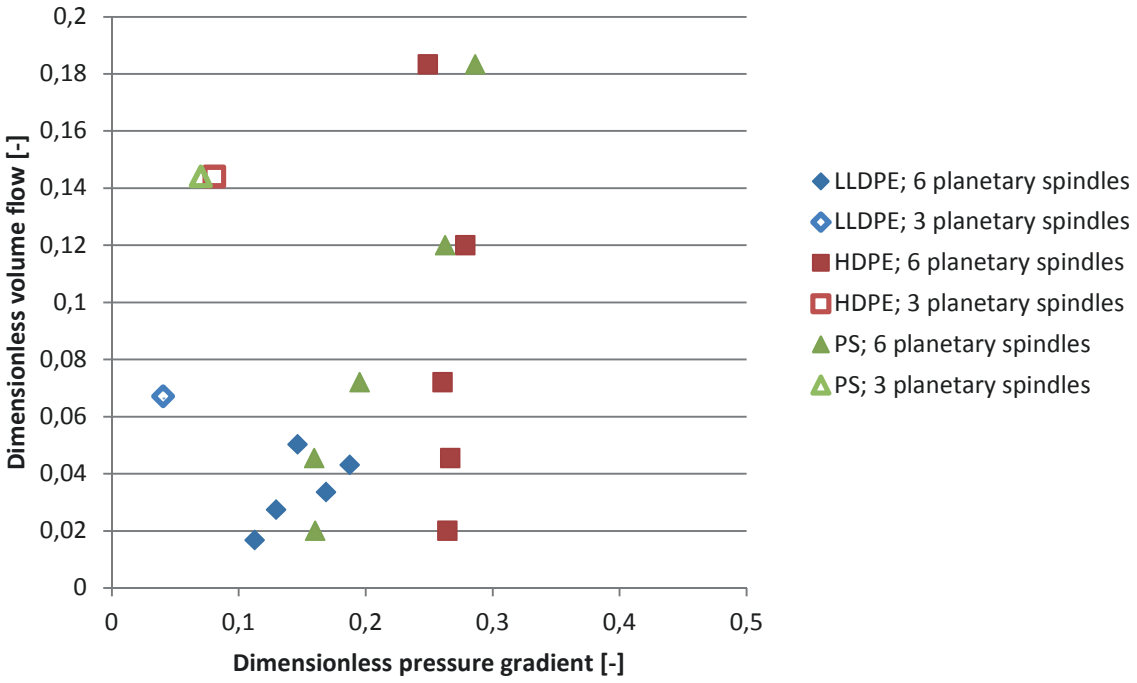

Figure 5: Dimensionless operating numbers calculated with experimental data

In order to find a relation between the dimensionless volume flow and the dimensionless pressure gradient a procedure according to [12] could be used. There the flow in complex mixing elements of twin screw extruder was modeled with a superposition of simple flow channels. First the intermeshing section channels are observed. For rectangular channels the melt transporting can be described by Equation 8 to 10.

$$\pi_{\dot{V},mesh} = \frac{\dot{V}_{mesh}}{\frac{1}{2} \cdot h_{mesh} \cdot b_{mesh} \cdot v_z} \tag{8}$$

$$\pi_{p,mesh} = \frac{\Delta p}{\Delta z} \cdot \frac{h_{mesh}^{n+1}}{6 \cdot K \cdot v_z^n} \tag{9}$$

$$\pi_{\dot{V},mesh} = A_{mesh} + B_{mesh} \cdot \pi_{p,mesh} \tag{10}$$

With the parameters A_{mesh} und B_{mesh} flow exponent and geometry influences can be considered. For the large channel an analogous approach can be used

$$\pi_{\dot{V},sub} = \frac{\dot{V}_{sub}}{\frac{1}{2} \cdot h_{sub} \cdot b_{sub} \cdot v_{MS}} \tag{11}$$

$$\pi_{p,sub} = \frac{\Delta p}{\Delta z} \cdot \frac{h_{sub}^{n+1}}{6 \cdot K \cdot v_{MS}^n} \tag{12}$$

$$\pi_{\dot{V},sub} = A_{sub} + B_{sub} \cdot \pi_{p,sub} \tag{13}$$

where v_{MS} is the rotation speed of the main spindle. In equation 8 and 12 $\dot{V}_{mesh}$ and $\dot{V}_{sub}$ are unknown, so the equations cannot be solved in this form. To address this problem equation 8 and equation 11 are transformed for the volume flow and introduced into equation 4 to get

$$\dot{V} = (\pi_{\dot{V},mesh} \cdot \frac{1}{2} \cdot h_{mesh} \cdot b_{mesh} \cdot v_z + \pi_{\dot{V},sub} \cdot \frac{1}{2} \cdot h_{sub} \cdot b_{sub} \cdot v_{MS}) \cdot n_{Pl} \tag{14}$$

.

By introducing this equation into equation 6 we get

$$\pi_{\dot{V}} = \pi_{\dot{V},mesh} + \pi_{\dot{V},sub} \cdot \frac{h_{sub} \cdot b_{sub} \cdot v_{MS}}{h_{mesh} \cdot b_{mesh} \cdot v_{mesh,z}} \tag{15}$$

and by introducing equation 10 and 13 into equation 15

$$\begin{aligned} \pi_{\dot{V}} &= A_{mesh} + B_{mesh} \cdot \pi_{p,mesh} + A_{sub} \cdot \frac{h_{sub} \cdot b_{sub} \cdot v_{MS}}{h_{mesh} \cdot b_{mesh} \cdot v_z} \\ &+ B_{sub} \cdot \pi_{p,sub} \cdot \frac{h_{sub} \cdot b_{sub} \cdot v_{MS}}{h_{mesh} \cdot b_{mesh} \cdot v_z} \end{aligned} \tag{16}$$

.

In the next step the pressure gradients have to be linked. By transforming equation 9 for the pressure gradient $\Delta p / \Delta z$ and introducing this into equation 12 we get

$$\pi_{p,sub} = \pi_{p,mesh} \cdot \frac{h_{sub}^{n+1} \cdot v_z^n}{h_{mesh,z}^{n+1} \cdot v_{MS}^n} \tag{17}$$

.

Finally by inserting this equation into equation 16 we get

$$\begin{aligned} \pi_{\dot{V}} &= A_{mesh} + B_{mesh} \cdot \pi_{p,mes} \\ &+ A_{sub} \cdot \frac{h_{sub} \cdot b_{sub} \cdot v_{MS}}{h_{mesh} \cdot b_{mesh} \cdot v_z} + B_{sub} \cdot \frac{h_{sub}^{n+2} \cdot v_z^{n-1} \cdot b_{sub}}{h_{mesh,z}^{n+2} \cdot v_{MS}^{n-1} \cdot b_{mesh}} \cdot \pi_{p,mesh} \end{aligned} \tag{18}$$

or transformed

$$\pi_{\dot{V}} = A_{mesh} + A_{sub} \cdot \frac{h_{sub} \cdot b_{sub} \cdot v_{MS}}{h_{mesh} \cdot b_{mesh} \cdot v_z} + \left(B_{mesh} + B_{sub} \cdot \frac{h_{sub}^{n+2} \cdot v_z^{n-1} \cdot b_{sub}}{h_{mesh,z}^{n+2} \cdot v_{MS}^{n-1} \cdot b_{mesh}} \right) \cdot \pi_{p,mesh} \tag{19}$$

.

To calculate the parameters A_{mesh}, A_{sub}, B_{mesh} and B_{sub} approximations of FEM Simulations are used in the literature [e.g. 3 or 12]. These approximations could principally be used for the PRE as well, but there is the problem that they are not valid for 45° angles as existing in the PRE or use slightly different dimensionless operating numbers. To find a solution for this problem, we started with setting the parameters A_{mesh}, A_{sub}, B_{mesh} and B_{sub} to a value of 1 and plotted the dimensionless operating numbers for different flow exponents and planetary spindle numbers (Figure 6).

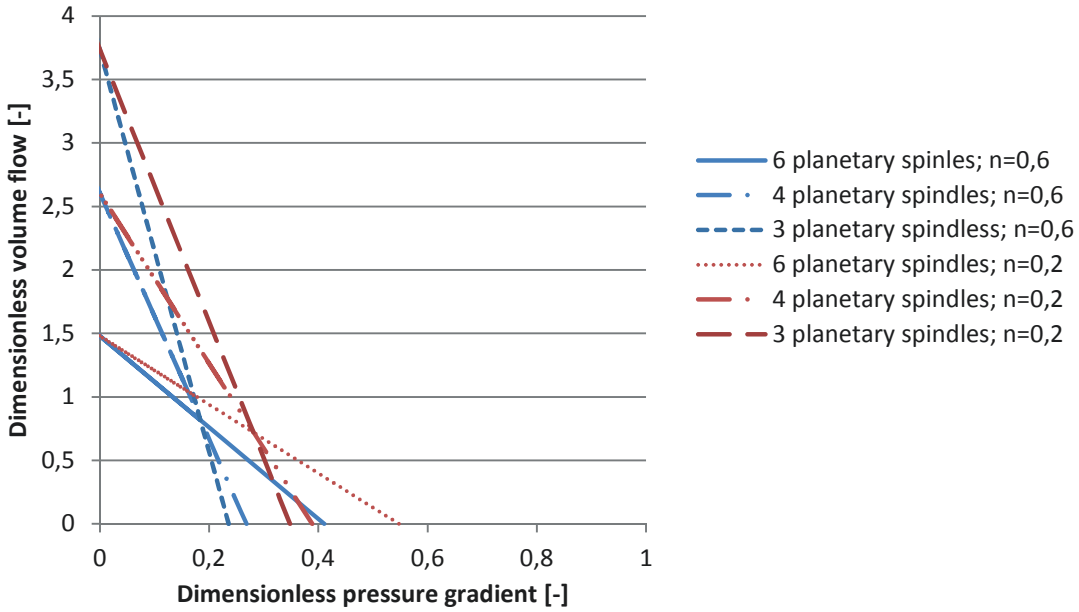

Figure 6: Dimensionless pressure-volume-flow graphs for different planetary counts and flow exponents

It can be seen that the dimensionless volume flow is overestimated especially for small pressure gradients. This problem increases while planetary spindle count decreases. Reason for that is a negligence of cross flow influences by setting A_{mesh}, A_{sub}, B_{mesh} and B_{sub} to a value of 1 and overrating the drag flow in the large channel.

Furthermore figure 6 shows that the curves for different planetary spindle counts intersect at one point that depends on the flow exponent n. At these points the sum of dimensionless pressure gradient and volume flow has exactly a value of 1. The intersection points can be described by equation 20:

$$\pi_{p,npl=i}(\pi_{\dot{V},npl=i}) = \pi_{p,npl=3}(\pi_{\dot{V},npl=3}) = \pi_{p,npl=6}(\pi_{\dot{V},npl=6}) = C = \frac{h_{mesh}^{n+1} \cdot v_{MS}^{n}}{h_{sub}^{n+1} \cdot v_{z}^{n}} \qquad (20)$$

To integrate the cross flow influence we now assume that the absolute volume flow of the PRE cannot exceed the maximal volume flow in the intermeshing section channels at a given pressure gradient. To fulfill this assumption the dimensionless volume flow at the intersection point has to be shifted to the y-axis with the factor C according to equation 21:

$$\pi_{\dot{V}} = A_{mesh} + A_{sub} \cdot \frac{h_{sub} \cdot b_{sub} \cdot v_{MS}}{h_{mesh} \cdot b_{mesh} \cdot v_z}$$
$$+ \left(B_{mesh} + B_{sub} \cdot \frac{h_{sub}^{n+2} \cdot v_z^{n-1} \cdot b_{sub}}{h_{mesh}^{n+2} \cdot v_{MS}^{n-1} \cdot b_{mesh}} \right) \cdot (\pi_{p,mesh} - C) \quad (21)$$

This leads to equation 22 with inserted values for the parameters A_{mesh}, A_{sub}, B_{mesh}, B_{sub} and C:

$$\pi_{\dot{V}} = 1 - \frac{h_{mesh}^{n+1} \cdot v_{MS}^{n}}{h_{sub}^{n+1} \cdot v_z^{n}} + \left(1 + \frac{h_{sub}^{n+2} \cdot v_z^{n-1} \cdot b_{sub}}{h_{mesh}^{n+2} \cdot v_{MS}^{n-1} \cdot b_{mesh}} \right) \cdot \pi_{p,mesh} \quad (22)$$

With equation 22 influences of the spindle count, spindle diameter, tooth height and flow exponent on the pressure build up of PRE can be described. Even the gearing angle influence is included through the velocity v_z. A comparison of calculated and measured dimensionless pressure gradients is shown in the Figures 7 and 8. There a descent agreement, especially under consideration of the simplifications used for modeling can be seen. The influence of the planetary spindle count is covered well and trends in the flow exponent influence can be reproduced.

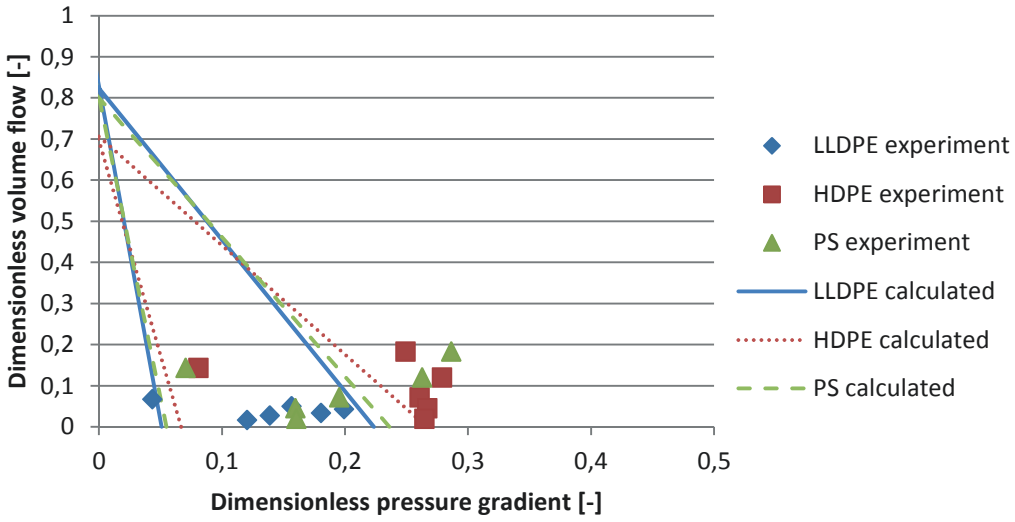

Figure 7: Shifted pressure-volume-flow graphs compared with experimental data

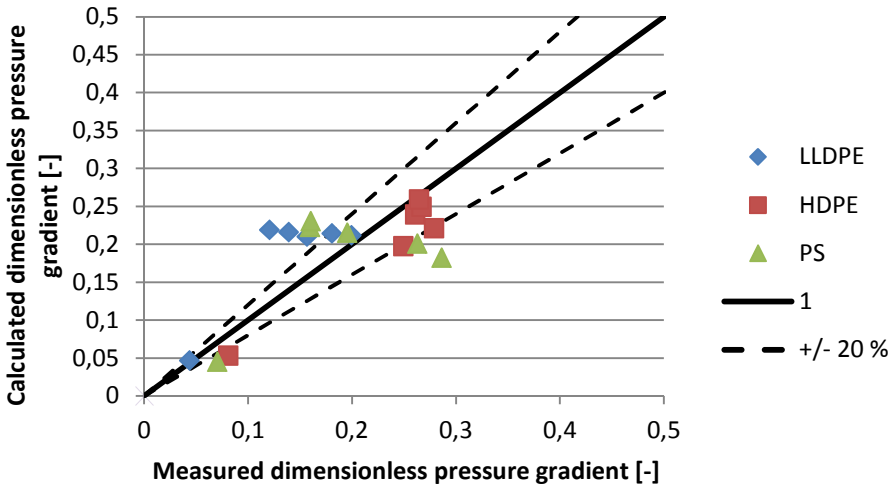

Figure 8: Comparison between measured and calculated dimensionless pressure gradients

5. CONCLUSION

The melt conveying in planetary roller extruders was analyzed in experimental research work. Based on the experiments the processes were described in dimensionless models. The developed models allow a simulation of the pressure build up in planetary roller extruders. The comparison between simulated results and experimental data shows a decent agreement, considering the simplifications made and the number of assumptions that were used to generate the model.

6. ACKNOWLDEDGMENTS

The results presented here were obtained in the research project “BA 1841/7-1”, which is supported by the German Research Foundation (DFG). Special thanks go to the DFG. Additional acknowledgements go to LyondellBasell, BASF and SABIC for supplying the polymer materials.

REFERENCES

[1] C. Rauwendaal, Polymer Extrusion, Carl Hanser Verlag, Munich, 2014.
[2] I. Radovanovic, Verarbeitung und Optimierung der Rezeptur von Wood Plastic Composites (WPC), PhD Thesis, University Osnabrück, 2006.
[3] M. Koch, Berechnung und Auslegung von Nutbuchsenextrudern, PhD Thesis, University of Paderborn, 1987.
[4] W. Szydlowski, J. L. White, “A Non-Newtonian Model of Flow in a Kneading Disk Region of a Modular Intermeshing Corotating Twin Screw Extruder”, Journal of Non-Newtonian Fluid Mechanics, 28, 1988.
[5] J. F. Agassant, P. Avenas , J.-Ph. Sergent, Polymer Processing: Principles and Modeling, Carl Hanser Verlag, Munich, 1991.
[6] J. Ansahl, Grundlagen zur Auslegung dichtkämmender Gleichdrall-Doppelschneckenextruder, PhD Thesis, University of Paderborn, 1993.
[7] J. L. White, H. Potente, Screw Extrusion, Carl Hanser Verlag, Munich, 2003.
[8] A. Limper, S. Seibel, G. Fattmann. “Compounding Unit Planetary Roller Extruder”, Macromolecular Materials and Engineering, 287, 2002

[9] A. Limper, S. Seibel, C.-J. Wefelmeier, M. Roth, “Intermeshing Spindles Improve the Mixing Action of Planetary-gear Extruders: Homogeneous Compounds”, Kunststoffe international, 2002/11
[10] J. Rudloff, K. Kretschmer, P. Heidemeyer, M. Bastian, M. Koch, “A physical – mathematical model describing the process behaviour of planetary roller extruders”, PPS 27 Proceedings, Marrakech, 2011, CD.
[11] J. Rudloff , M. Lang, K. Kretschmer, P. Heidemeyer, M. Bastian, M. Koch, “A mathematical model describing the solid conveying and melting behavior of planetary roller extruders”, PPS 29 Proceedings, Nuremberg, 2013, CD.
[12] K. Kretschmer, Untersuchung und Beschreibung des Prozess- und Mischverhaltens von Mischelementen für Gleichdrall-Doppelschneckenextruder, PhD Thesis, University of Paderborn, 2004.

CONTACTS

Dipl.-Ing. J. Rudloff j.rudloff@skz.de
Dipl.-Chem. M. Lang m.lang@skz.de
Dr.-Ing. K. Kretschmer k.kretschmer@skz.de
Dr.-Ing. P. Heidemeyer p.heidemeyer@skz.de
Prof. Dr.-Ing. M. Bastian m.bastian@skz.de
Prof. Dr.-Ing. habil. M. Koch michael.koch@tu-ilmenau.de

